Glutamate-induced internalization of $Ca_V1.3$ L-type Ca^{2+} channels protects retinal neurons against excitotoxicity

Fengxia Mizuno[1], Peter Barabas[2], David Krizaj[2] and Abram Akopian[1]

[1] Department of Ophthalmology, NYU Medical Center, New York, NY 10016, USA
[2] Departments of Ophthalmology and Physiology, and Moran Eye Institute, University of Utah School of Medicine, Salt Lake City, UT 84132, USA

Glutamate-induced rise in the intracellular Ca^{2+} level is thought to be a major cause of excitotoxic cell death, but the mechanisms that control the Ca^{2+} overload are poorly understood. Using immunocytochemistry, electrophysiology and Ca^{2+} imaging, we show that activation of ionotropic glutamate receptors induces a selective internalization of $Ca_v1.3$ L-type Ca^{2+} channels in salamander retinal neurons. The effect of glutamate on $Ca_v1.3$ internalization was blocked in Ca^{2+}-free external solution, or by strong buffering of internal Ca^{2+} with BAPTA. Down-regulation of L-type Ca^{2+} channel activity in retinal ganglion cells by glutamate was suppressed by inhibitors of dynamin-dependent endocytosis. Stabilization of F-actin by jasplakinolide significantly reduced the ability of glutamate to induce internalization suggesting it is mediated by Ca^{2+}-dependent reorganization of actin cytoskeleton. We showed that the $Ca_v1.3$ is the primary L-type Ca^{2+} channel contributing to kainate-induced excitotoxic death of amacrine and ganglion cells. Block of $Ca_v1.3$ internalization by either dynamin inhibition or F-actin stabilization increased vulnerability of retinal amacrine and ganglion cells to kainate-induced excitotoxicity. Our data show for the first time that $Ca_v1.3$ L-type Ca^{2+} channels are subject to rapid glutamate-induced internalization, which may serve as a negative feedback mechanism protecting retinal neurons against glutamate-induced excitotoxicity.

(Received 10 September 2009; accepted after revision 26 January 2010; first published online 1 February 2010)
Corresponding author A. Akopian: Department of Physiology and Neuroscience, NYU Medical Center, 550 First Ave, New York, NY 10016, USA. Email: aa3@nyu.edu

Abbreviations CytD, cytochalasin D; DIP, dynamin inhibitory peptide; iGluR, ionotropic glutamate receptor; LTCC, L-type Ca^{2+} channel; mGluR, metabotropic glutamate receptor; RGC, retinal ganglion cell.

Introduction

Glutamate is the major excitatory neurotransmitter in the central nervous system. In the vertebrate retina, glutamate is released from photoreceptors and bipolar cell terminals and exerts its actions by activating postsynaptic ionotropic (iGluR) and/or metabotropic (mGluR) receptors that are expressed in most, if not all, retinal cells (reviewed by Thoreson & Witkovsky, 1999). Overstimulation of glutamate receptors (GluRs), however, can lead to excitotoxic neuronal injury and death (Choi, 1988). Although the molecular basis of excitotoxic action of glutamate is not well understood, a strong relationship between glutamate-triggered neuronal injury and excessive Ca^{2+} influx has been established (Arundine & Tymianski, 2003). The major Ca^{2+} entry pathways contributing to the glutamate-induced rise in $[Ca^{2+}]_i$ of central and retinal neurons are Ca^{2+}-permeable AMPA/kainate and NMDA receptors (NMDARs), as well as voltage-gated Ca^{2+} channels, which are indirectly activated by glutamate-induced depolarization. Consistent with this, blockers of voltage-gated L-type Ca^{2+} channels (LTCC) can be neuroprotective by reducing the amount of Ca^{2+} loading incurred by GluR stimulation (Sucher *et al.* 1997; Sattler & Tymianski, 2001; Uemura & Mizota, 2008).

In the vertebrate retina, Ca^{2+} entry through voltage-gated LTCCs plays a fundamental role in many physiological processes including neurotransmitter release, activation of intracellular signalling, regulation of excitability and gene expression (reviewed by Akopian & Witkovsky, 2002). Three subtypes of LTCC, $Ca_V1.2$, $Ca_V1.3$ and $Ca_V1.4$, with different biophysical and pharmacological properties and different cellular distribution are expressed in the mammalian retina (Kamphuis & Hendriksen, 1998; Taylor & Morgans, 1998; Henderson *et al.* 2001). The $Ca_v1.4$ subtype has been localized primarily to rod and bipolar cell terminals, and its role in the synaptic transmission and in incomplete congenital stationary night blindness has

DOI: 10.1113/jphysiol.2009.181305

been well established (Strom *et al.* 1998; Morgans, 1999; Bech-Hansen *et al.* 2000). Although $Ca_v1.2$ and $Ca_v1.3$ subtypes have been localized to both synaptic and nuclear layers encompassing cell bodies and processes of ganglion, amacrine and Müller cells (Firth *et al.* 2001; Henderson *et al.* 2001; Cristofanilli *et al.* 2007), their role in the retinal function is unclear. In the present study we tested the hypothesis that activation of glutamate receptors causes a rapid internalization of $Ca_v1.3$ LTCCs. Our results suggest that LTCC internalization acts synergistically with the glutamatergic input to regulate the amount of the excitatory drive of retinal ganglion cells (RGCs). We also provide evidence that this mechanism can compensate for overstimulation of GluRs in RGCs, resulting in a decrease in the magnitude of voltage-activated Ca^{2+} elevations. This serves as a negative-feedback mechanism, which provides an adaptational component to the inner retinal circuitry as well as protection against glutamate excitotoxicity.

Methods

Animals

The handling and the maintenance of animals met the National Institutes of Health guidelines and were approved by Institutional Care and Use Committee at NYU School of Medicine. The number of animals used and their suffering were minimized. Salamanders (*Ambystoma tigrinum*) were anaesthetized using tricaine methanosulfonate (100 mg ml^{-1}) until the animal no longer reacted to tactile stimulation, then were decapitated and double pithed.

Electrophysiology

The general procedures for preparing dissociated cells and slices of salamander retina for patch clamp and immunocytochemistry have been published (Cristofanilli *et al.* 2007). Briefly, salamander eyes were cut in half, and the retina was dissected out either for preparation of dissociated cells or for retinal slices. The normal Ringer solution contained (in mM): NaCl 100, KCl 2.5, $CaCl_2$ 2, $MgCl_2$ 2 and Hepes 10, adjusted to pH 7.5 with NaOH. Standard internal solution contained (in mM): potassium gluconate 100, $MgCl_2$ 2, $CaCl_2$ 0.2, EGTA 2, Hepes 10, ATP 2 and GTP 0.1, adjusted to pH 7.3. The precise composition of the intracellular and bath solutions varied according to the requirements of the experiment. Whole-cell voltage-gated Ca^{2+} currents (I_{Ca}) were recorded using Patchmaster software and an EPC-10 amplifier (HEKA Electronic, Germany) and analysed with Igor Pro5 software. Capacitance and series resistances were compensated automatically. Membrane currents were sampled at 5 kHz and filtered at 1.0 kHz. A standard voltage protocol was used to elicit voltage-dependent I_{Ca} in the presence of TTX (1 μM) and TEA (20 mM, replacing equimolar NaCl) in bath solution to block voltage-gated Na^+ and K^+ currents, respectively. In addition, Ω-conotoxin GVIA (800 nM) and Ω-agatoxin IVA (1 μM) were included in the bath solution to block N- and P/Q-type Ca^{2+} currents, respectively. Unless otherwise noted, I_{Ca} was recorded with 5–10 mM Ca^{2+} (but not Ba^{2+}) in the external solution as a charge carrier to allow full expression of Ca^{2+}-dependent processes. Currents were recorded with low-resistance electrodes (5–6 MΩ), filled with pipette solution consisting of (mM): 100 CsCl, 10 KCl, 0.5 $CaCl_2$, 2 $MgCl_2$, 0.5 EGTA, 2 ATP, 0.1 GTP and 10 Hepes, buffered to pH 7·4 with KOH. Summary data are presented as mean ± S.E.M. Statistical comparisons among groups were performed with Student's unpaired *t* test and differences were considered significant at the $P < 0.05$ level.

Immunocytochemistry

The detailed procedure for labelling dissociated cells and slices of salamander retina for different Ca^{2+} channel subtypes is similar to those described previously (Cristofanilli *et al.* 2007). Briefly, isolated retinas were incubated for 1 h at room temperature (RT) with papain solution (14 U ml^{-1}, Worthington Biochemicals, Lakewood, NJ, USA) in 14 ml of 0.5 mM calcium Ringer solution containing 6 mg cysteine, 1 mM sodium pyruvate, 16 mM D-glucose and 1.1 mM EDTA. After rinses in normal Ringer solution, retinas were triturated and cells plated on poly-L-lysine-coated coverslips to settle for 30–40 min before treatments.

To trigger internalization, cells were exposed for 5–10 min to glutamate, kainate or NMDA in normal external solution prior to fixing and labelling with anti-$Ca_v1.2$ or anti-$Ca_v1.3$ antibodies. To block endocytosis, cells were pre-incubated for 1 h with 50 μM myristoylated dynamin-inhibitory peptide (Tocris, Ellisville, MO, USA). For immunostaining of $Ca_v1.3$ and $Ca_v1.2$ channels, cells were permeabilized with 0.1% Triton X-100 for 5 min in PBS, pre-incubated in blocking solution (4% donkey serum 0.1% Triton X-100 in PBS) for 1 h at RT then incubated overnight at 4°C with polyclonal rabbit anti-$Ca_v1.3$ (Chemicon, Temecula, CA, USA; at 1:200) or anti-$Ca_v1.2$ (Alomone Labs, Israel; at 1:200) antibodies diluted 1:200 in blocking solution. Cells were rinsed three times in PBS and incubated with corresponding secondary antibodies diluted in blocking solution: Cy3 (Jackson Immunoresearch, West Grove, PA, USA; at 1:200); or Alexa Fluor 488, (Molecular Probes, Eugene, OR, USA; at 1:1000). Cells were

then rinsed three times in PBS and coverslipped with Prolong Gold Antifade Mounting Medium (Invitrogen, Carlsbad, CA, USA) and observed with a confocal laser-scanning microscope (Nikon Eclipse C-1, Nikon, Japan). Specificity of the antibody for salamander retina was tested by (a) Western blot analysis (Cristofanilli *et al.* 2007), (b) omitting the primary antibody, and (c) pre-absorbing the primary antibodies with their respective control peptides (online Supplementary Fig. 1). For pre-absorption experiments, 1 μg of anti-$Ca_v1.3$ or anti-$Ca_v1.2$ antibodies were incubated for 1 h with 1 μg of corresponding control peptides at room temperature (according to the manufacturer's instructions) before making the final dilutions. We also demonstrated that $Ca_v1.3$ antibody recognizes the intended channel by utilizing a $Ca_v1.3$ knockout mouse (Busquet *et al.* 2009). Images of a single focal plane through the centre of the cells were acquired using 60× or 100× oil-immersion objective lens and EZ-C1 (Nikon) software. Changes in the subcellular distribution of $Ca_v1.2$ and $Ca_v1.3$ channels were assessed by measuring separately the optical fluorescence densities for the total (F_t) and the cytosolic (F_c) areas, using Metamorph software (Universal Imaging Co., Downington, PA, USA). To control for day-to-day variations in staining intensity, treated specimens always were compared with controls prepared the same day under identical fixation, permeabilization, staining and microscopy conditions. Control experiments consist of omitting the primary antibody, using knockout mice animals, and pre-absorbing the primary antibodies with their respective control peptides. For quantification, the membrane fluorescence (F_m) was defined as the difference between F_t and F_c, and the degree of internalization was assessed by measuring the ratio of F_c/F_m (Tombler *et al.* 2006). Fluorescence intensity profiles were obtained by scans of pixel intensity along a line drawn through the cell perikarya by using Metavue software (Universal Imaging Co.). All data are presented as mean ± S.E.M. Levels of significance were assessed using Student's paired *t* test with $P < 0.05$ considered as significant.

Assessment of cell death

Eyecups of salamander were treated with agonists at various concentrations in normal Ringer solution, for 30–60 min, incubated in agonist-free medium for 4–6 h, and cell viability was evaluated by a live/dead assay (Molecular Probes). Samples were loaded with the fluorescent dyes calcein-AM (2 μM) and ethidium homodimer (4 μM), for 30 min in darkness. After washing out excess dyes with normal Ringer solution, eyecups were cryoprotected in 20% sucrose dissolved in PBS at 4°C overnight. Cryostat sections of 15–18 μm were cut and fluorescence images were obtained with a confocal microscope. Live cells were detected by the presence of ubiquitous intracellular esterase activity, determined by the enzymatic conversion of the virtually non-fluorescent cell-permeant calcein AM to green fluorescence. Dead or damaged cells were identified by the uptake of ethidium homodimer-1, a red nuclear dye that is taken up only by damaged or dying cells with permeant membranes. For each treatment group, 15–30 retinal sections (from 3 independent experiments) comparable in size and location were processed. The number of dead cells was counted manually in several visual fields, averaged per slice and plotted as mean ± S.E.M. Statistical significance between groups was determined by one-way ANOVA followed by Tukey *post hoc* test. The differences were considered significant if $P < 0.05$.

Results

Glutamate induces selective internalization of $Ca_v1.3$ channels in salamander retinal neurons

To investigate whether activation of GluRs alters the number of surface-expressed $Ca_v1.3$ channels on plasma membrane, dissociated retinal neurons were stimulated for 5 min with 100 μM glutamate prior to fixation and subsequent immunostaining with anti-$Ca_v1.3$ antibody.

Parallel immunostaining was performed on control cells incubated in normal Ringer solution. The analysis presented below is confined to non-photoreceptor and non-bipolar cells, which were easily identifiable by their morphology, and excluded based on the distinct shape of their ellipsoids and Landolt's clubs (Szikra & Krizaj, 2006). As a criterion for selecting ganglion cells, we used a minimum cell body diameter of 15 μm. Confocal immunofluorescence images through the perikarya of presumed amacrine and ganglion cells show that under control conditions, $Ca_v1.3$ labelling appeared as puncta outlining the cell somas, indicative of a surface localization (Fig. 1*A* and *A*′). Upon exposure to glutamate, the fluorescence signal appeared to be more intense in the cytoplasm (Fig. 1*B* and *B*′), suggesting that activation of GluRs induced $Ca_v1.3$ channel internalization. For quantification, we measured F_t and F_c for each cell, and calculated the membrane intensity per pixel as $F_m = F_t - F_c$ (details in Methods). The ratio of F_c/F_m was used to evaluate internalization (Tombler *et al.* 2006). In this series of experiments, glutamate increased the mean F_c/F_m ratio from 0.62 ± 0.09 to 1.33 ± 0.12 ($n = 50$, $P < 0.05$). The F_c/F_m ratios for control and glutamate-treated cells are presented in Fig. 1*E* and *F*.

In contrast to its prominent effect on $Ca_v1.3$ distribution, glutamate had a relatively small effect on subcellular distribution of $Ca_v1.2$ channels. Confocal

images of retinal cells labelled with anti-$Ca_v1.2$ antibodies in control Ringer solution (Fig. 1*C* and *C*′), and after exposure to glutamate (Fig. 1*D* and *D*′), showed a significant but much smaller difference in $Ca_v1.2$ immunolabelling. A slight increase in F_c/F_m (from 0.57 ± 0.04 to 0.71 ± 0.05) (Fig. 1*F*), suggests a potential yet minor effect of glutamatergic stimulation on internalization of $Ca_v1.2$. Intensity profiles (insets in upper panels) corroborate these data, suggesting that in salamander retinal neurons, LTCCs undergo subtype-selective modulation by glutamate.

Type of GluR responsible for $Ca_v1.3$ internalization

The effect of glutamate on the plasma membrane–cytosolic switch of $Ca_v1.3$ immunofluorescence was attenuated in the combined presence of CNQX (10 μM) and AP-7 (100 μM), indicative of ionotropic AMPA and/or NMDA receptor stimulation. To determine which subtype of iGluR is responsible for internalization of $Ca_v1.3$, cells were exposed either to kainate (100 μM) or to NMDA (100 μM, in Mg^{2+}-free Ringer solution). In these experiments, $CdCl_2$ (100 μM) was added to the Ringer solution to exclude contribution from voltage-gated Ca^{2+} channels. Both agonists induced a qualitatively similar but quantitatively lesser effect on $Ca_v1.3$ distribution compared with glutamate (Fig. 2*A*–*C*). Quantification revealed an increase in F_c/F_m by kainate and NMDA from a control value of 0.7 ± 0.03 ($n = 50$) to 1.9 ± 0.3 ($n = 25$, $P < 0.05$) and 2.2 ± 0.4 ($n = 50$, $P < 0.05$), respectively, compared with 2.6 ± 0.11 ($n = 70$, $P < 0.05$) induced by glutamate application.

The modest effect of NMDA compared to glutamate might be associated with the partial blockage of NMDARs by Cd^{2+}, which at a concentration of 1 mM was shown to suppress NMDA-evoked currents in rabbit retinal amacrine cells (Zhou & Fain, 1995).

To determine whether internalization can be triggered by tonic electrical activity, dissociated cells were exposed for 5 min to 30 mM KCl in the presence of the N/P/Q

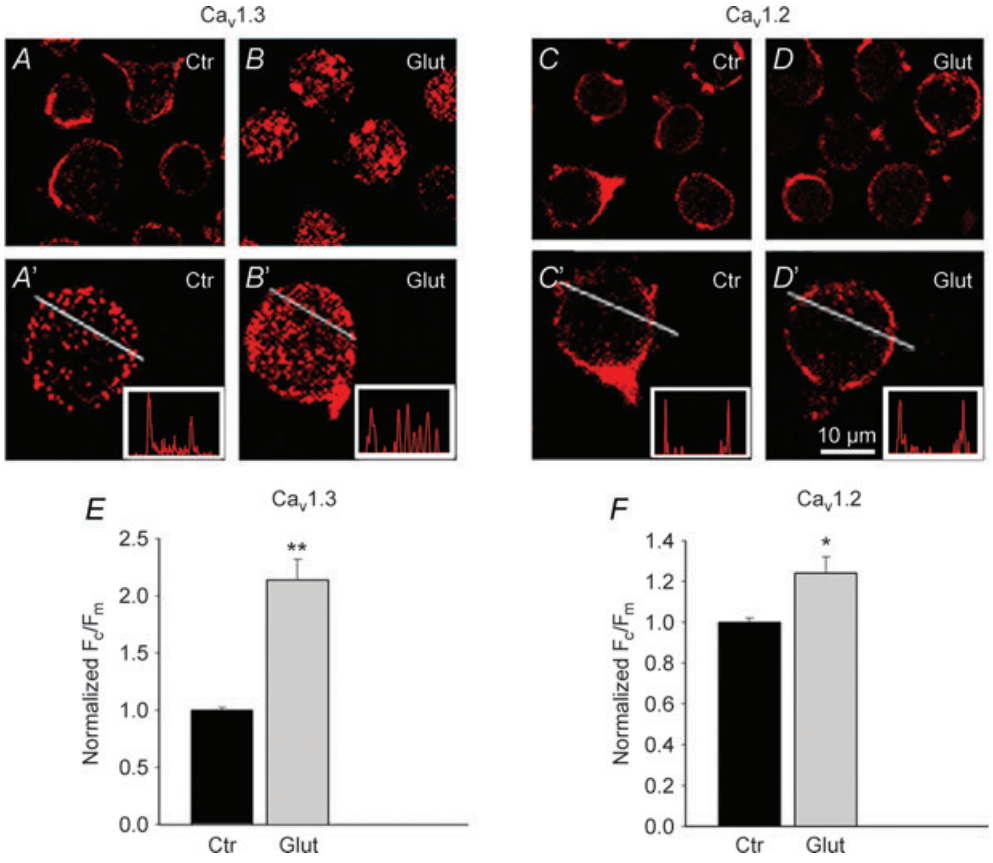

Figure 1. Glutamate induces selective internalization of Cav1.3 channels in salamander retinal neurons
Confocal immunofluorescence images of cells incubated in normal Ringer solution (*A*, *A*′, *C*, *C*′), exposed for 5 min to 100 μm glutamate (*B*, *B*′, *D*, *D*′), then fixed and labelled for $Ca_v1.3$ or $Ca_v1.2$. Representative cells from 3 independent experiments were mounted in upper panels. Lower panels show magnified images of individual cells from corresponding upper panels. Glutamate induced internalization of $Ca_v1.3$ (B and B′) but had no significant effect on subcellular distribution of $Ca_v1.2$ (*D* and *D*′). *E* and *F*, the degree of internalization is presented as F_c/F_m, normalized to untreated cells. Bars: mean ± S.E.M. ($n = 15$–30; $P < 0.01$).

channel antagonist ω-conotoxin MVIIC (1 μM). This protocol caused robust internalization of $Ca_v1.3$ channels (Fig. 2*D*), increasing F_c/F_m to 4.2 ± 0.3 ($n = 30$, $P < 0.05$). The normalized values of F_c/F_m are presented in Fig. 2*E*. These data suggest that in salamander retinal neurons, internalization of LTCC is activity dependent. Although the exact identity of targeted cells was not established in these studies, the sensitivity of $Ca_v1.3$ distribution to NMDA suggests an involvement of third-order (amacrine and/or ganglion) retinal neurons (Shen & Slaughter, 1998). GluR agonists had no effect on subcellular distribution of $Ca_v1.3$ channels in photoreceptors, consistent with the absence of glutamate-evoked $[Ca^{2+}]_i$ responses in salamander photoreceptors ($n = 20$, Supplementary Fig. 2).

We next tested whether $Ca_v1.3$ internalization can be induced by activation of mGluRs. The predominant mGluR in salamander ganglion cells has been identified as a group III mGluR, activation of which stimulates Ca^{2+} release from IP_3-sensitive stores (Shen & Slaughter, 1998). L-AP4 (100 μM), an agonist of group III metabotropic receptors, failed to induce detectable internalization. Thus, the normalized (to control) value of F_c/F_m in the presence of L-AP4 was $0.97 + 0.04$ ($P > 0.5$, $n = 25$), indicating that activation of iGluRs, rather than mGluRs, is responsible for glutamate-induced internalization (Supplementary Fig. 3).

Glutamate-induced internalization depends on dynamin activity

There are several different mechanisms by which cells internalize receptor and channel proteins into transport vesicles derived from the plasma membrane. Clathrin-mediated endocytosis, which strictly depends on GTPase activity of dynamin, is the best characterized mechanism for the removal of receptor and channel proteins from the plasma membrane into the cell interior (reviewed by Le Roy & Wrana, 2005).

To determine whether the internalization of $Ca_v1.3$ channels depends on dynamin activity, we used a myristoylated dynamin-inhibitory peptide (DIP) that blocks endocytosis of receptor and channel proteins by interfering with the binding of amphiphysin with dynamin (Wigge *et al.* 1997). Dissociated cells were incubated for 1 h in Ringer solution without (Fig. 3*A* and *C*) or with 50 μM DIP (Fig. 3*B* and *D*), prior to glutamate or NMDA exposure. Cells were then washed, fixed and labelled for $Ca_v1.3$.

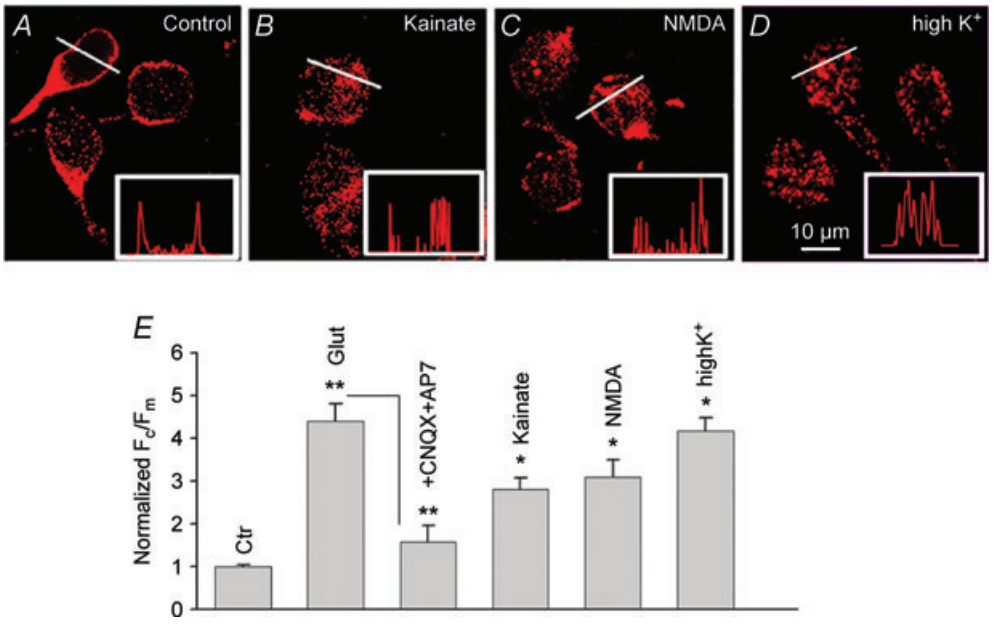

Figure 2. Activation of ionotropic glutamate receptors or prolonged depolarization induces internalization of $Ca_v1.3$ channels in salamander third-order retinal cells
Confocal immunofluorescence images of cells labelled for $Ca_v1.3$ in normal Ringer solution (*A*), after 5 min exposure to 100 μM kainate (*B*), 100 μM NMDA (in Mg^{2+}-free external solution) (*C*), or 30 mM KCl (*D*). $CdCl_2$ (100 μM) was used together with glutamate receptor agonists to exclude contribution of Ca^{2+} entry through voltage-gated channels. Intensity profiles (insets) along the white lines show changes in membrane and cytoplasmic labelling. *E*, the total integrated intensity (F_t) and cytoplasmic intensity (F_c) for each cell was measured, and the membrane intensity per pixel was calculated as $F_m = F_t - F_c$. Degree of internalization assessed as a ratio of F_c/F_m. Bars represent the normalized (to control (Ctr)) $F_c/F_m \pm$ S.E.M. ($n = 20$–40, $P < 0.05$).

Intensity profiles (insets) and quantitative analysis of F_c/F_m ratios (Fig. 3*E*) show that DIP greatly suppressed both glutamate- and NMDA-induced internalization. The effect of DIP was specific, as its inactive form (DIPctr) failed to suppress glutamate-induced internalization. These data suggest that glutamate-induced internalization of $Ca_v1.3$ is mediated by clathrin-dependent endocytosis.

Ca^{2+} entry from the extracellular space is essential for glutamate-induced internalization

Activation of iGluRs and mGluRs in third-order retinal neurons induces a large Ca^{2+} influx from extracellular space and release from IP_3-sensitive internal Ca^{2+} stores, respectively (Shen & Slaughter, 1998; Akopian *et al.* 2006; Hartwick *et al.* 2008). To determine whether Ca^{2+} plays a role in the glutamate-induced internalization, retinal cells were incubated for 10–15 min in Ringer solution in either the absence (Fig. 4*A*) or presence (Fig. 4*B*) of 10 μM BAPTA-AM, prior to glutamate exposure. Cells were subsequently labelled for $Ca_v1.3$ and processed to assess the internalization. Whereas treatment with BAPTA-AM alone had no effect on $Ca_v1.3$ distribution, it prevented glutamate-induced internalization. This finding suggests that $[Ca^{2+}]_i$ elevation within the cytosol represents the paramount stimulus for $Ca_v1.3$ internalization. In cells treated with BAPTA-AM and exposed to glutamate, the F_c/F_m ratio of 0.77 ± 0.13 ($n = 40$; $P > 0.5$) was not significantly different from 0.69 ± 0.04, observed in control cells.

We next examined whether Ca^{2+} influx from extracellular space or its release from internal stores, e.g. by Ca^{2+}-induced Ca^{2+} release (CICR), plays a role in $Ca_v1.3$ internalization. Depletion of IP_3-sensitive Ca^{2+} stores by 1 μM thapsigargin or antagonism of store-operated Ca^{2+} entry by 2-aminoethoxydiphenyl borate (100 μM 2-APB; Maruyama *et al.* 1997; Szikra *et al.* 2008), had no effect on glutamate-induced internalization ($n = 8$, $P > 0.3$, not shown). To test the role of Ca^{2+} entry, dissociated cells were exposed to glutamate in Ca^{2+}-free external solution (Fig. 4*C*). The effect of glutamate was attenuated in the absence of external Ca^{2+}. Thus, in the presence of glutamate the F_c/F_m ratio in Ca^{2+}-free solution fell to 1.4 ± 0.15 ($n = 25$, $P < 0.05$) from 3.1 ± 0.4 in normal Ringer solution (Fig. 4*D*). These data indicate that Ca^{2+} entry via voltage-gated Ca^{2+} channels and/or iGluR-activated channels rather than its release from internal stores is essential for triggering internalization.

Correlation between internalization and inhibition of L-type Ca^{2+} current by glutamate

While the immunocytochemical data demonstrate glutamate-induced internalization of $Ca_v1.3$ LTCC, the

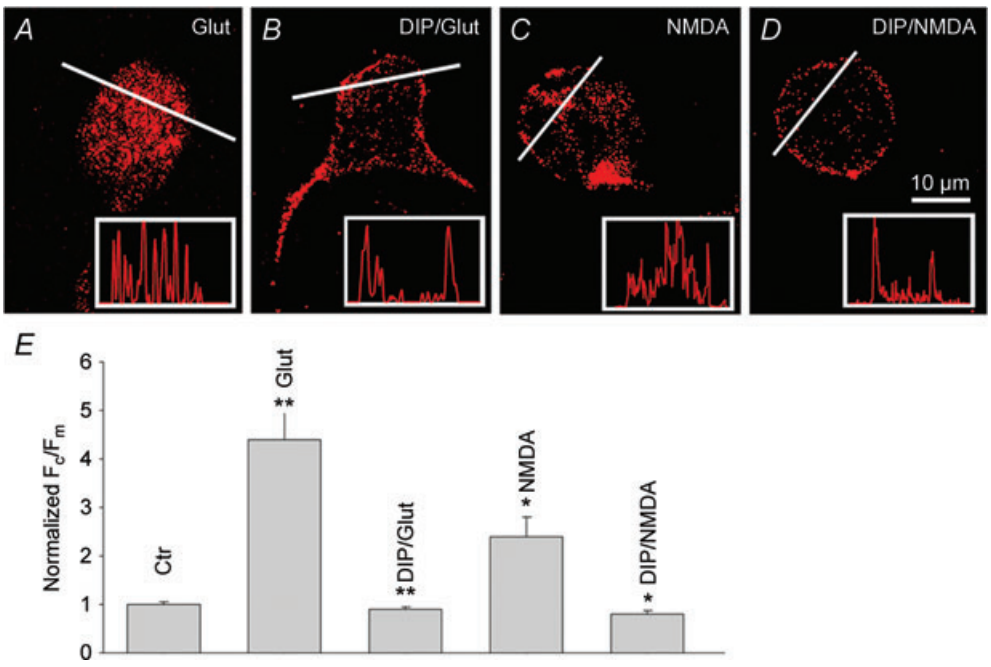

Figure 3. Internalization of $Ca_v1.3$ channels depends on dynamin activity
Salamander retinal cells were incubated either in normal Ringer solution (*A* and *C*), or Ringer solution containing 50 μM DIP (*B* and *D*), prior to exposure for 5 min to glutamate or NMDA. Cells were then fixed and labelled for $Ca_v1.3$. Intensity profiles for corresponding cells are shown in insets. *E*, the bar graph shows no significant difference in F_c/F_m ratio in control cells *vs.* DIP-treated cells exposed to glutamate or NMDA. Bars represent mean $F_c/F_m \pm$ S.E.M. ($n = 20$–30, $P < 0.01$).

following key questions remain to be answered: (i) Are these the same channels that are responsible for Ca^{2+} entry during cell depolarization, and (ii) Is internalization accompanied by downregulation of LTCC activity? To address these questions, the inhibitory action of glutamate on L-type I_{Ca} was measured in control and DIP-treated salamander retinal slices. Whole-cell Ca^{2+} currents were recorded from RGCs in which N- and P/Q-channels were suppressed by a cocktail consisting of ω-conotoxin GVIA (800 nM) and ω-agatoxin IVA (1 μM) in the bath solution. Patch pipette solution contained 1 μM thapsigargin and 100 μM 2-APB to suppress contributions from Ca^{2+} stores and store-operated channels, respectively. We used Ca^{2+} rather than Ba^{2+} as charge carrier, because Ba^{2+} obscures functionally important interactions between Ca^{2+} and Ca^{2+}-dependent intracellular signalling.

In control slices, application of 100 μM glutamate reduced L-type I_{Ca} by $33 \pm 3\%$ ($n = 16$, $P < 0.05$), without altering the voltage dependence of I–V relationships or current kinetics (Fig. 5*A* and *C*).

The inhibitory action of glutamate could not be relieved by large depolarizing pre-pulses (500 ms to +80 mV, $n = 3$) that usually used to relieve voltage-dependent inhibition of I_{Ca} by activation of G protein-coupled receptors, suggesting this phenomenon was independent of transmembrane voltage. In addition, an overlap between normalized activation curves obtained before and after glutamate application was observed, indicating that glutamate-induced suppression of I_{Ca} did not result from a shift in the channel's voltage dependence (not shown). The inhibitory action of glutamate was suppressed by 10 mM BAPTA in the patch pipette solution (data not shown). Combined, these data indicate that activation of GluRs reduces the activity of LTCCs in RGCs in a Ca^{2+}-dependent and voltage-independent manner, which is in agreement with earlier reports (Taschenberger & Grantyn, 1998; Shen & Slaughter, 1998).

Glutamate-induced reduction in Ca^{2+} channel activity may arise from removal of plasma membrane channels by the endocytic pathway (Jarvis & Zamponi, 2007). To test this possibility, the inhibitory action of glutamate on I_{Ca} was examined in slices pre-treated with DIP. Block of endocytosis by DIP suppressed the inhibitory action of glutamate by ~60% from a mean inhibition of $33 \pm 3\%$ to $12 \pm 4\%$ ($n = 8$, $P < 0.05$) (Fig. 5*B* and *C*). The effect of DIP was specific, as its inactive form (DIP_{ctr}) was ineffective (Fig. 5*B*). Confocal immunofluorescence images of $Ca_v1.3$-labelled cells and intensity profiles under corresponding conditions are illustrated in insets. Quantification showed good correlation between glutamate-induced inhibition of I_{Ca} (Fig. 5*D*) and internalization of $Ca_v1.3$ channels (Fig. 5*E*). The residual $12 \pm 4\%$ inhibition of I_{Ca} in DIP-treated cells although small was statistically significant, suggesting that

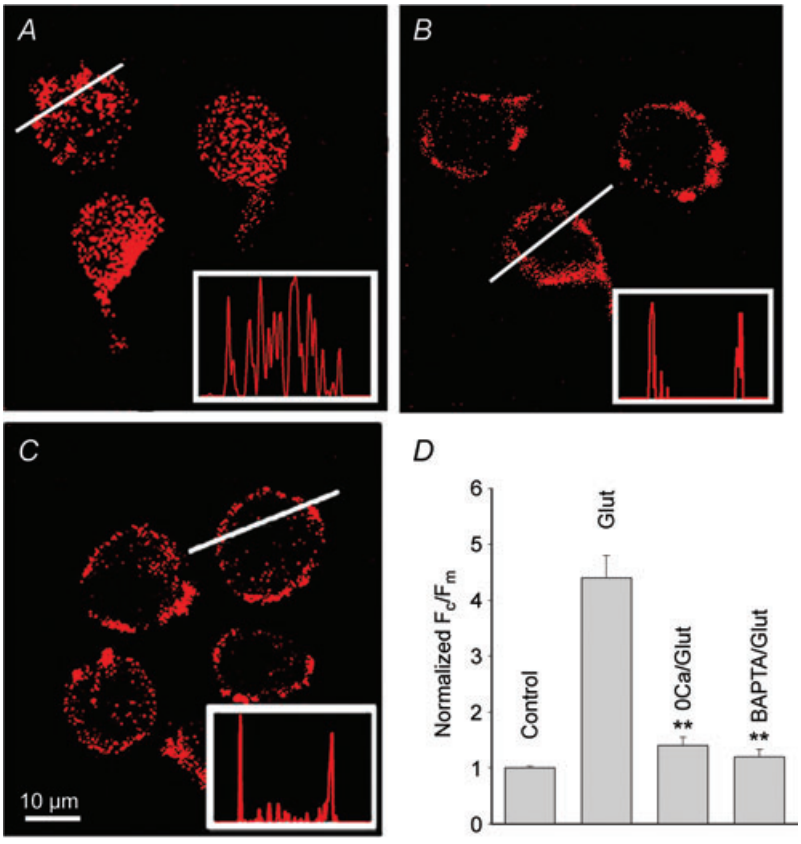

Figure 4. Calcium influx is essential for glutamate-induced internalization
Glutamate-induced internalization of $Ca_v1.3$ channels observed in normal Ringer solution (2 mM $CaCl_2$) (*A*), was prevented by pre-treatment of cells for 10 min with 10 μM BAPTA-AM (*B*), or by removal of Ca^{2+} from external solution (*C*). Intensity profiles are shown in insets. *D*, the bar graph represents normalized (to control) F_c/F_m values obtained under different experimental conditions. Data values represent mean $F_c/F_m \pm$ S.E.M. ($n = 20$–50, $P < 0.001$).

additional mechanisms, acting independently of endocytosis, may also be involved.

Role of the actin cytoskeleton in the glutamate-induced internalization

We next addressed the potential mechanism underlying the Ca^{2+}-dependent internalization of $Ca_v1.3$ channels by glutamate. Ca^{2+} influx could induce LTTC internalization through actin depolymerization which would facilitate dissociation of channel proteins from their anchoring sites at the plasma membrane (Lanzetti, 2007). Cells were incubated for 30 min prior to glutamate exposure with Ringer solution containing 10 μM of the F-actin stabilizer jasplakinolide (Fig. 6*A*, Jasplk/Glut). Cells were subsequently washed, labelled for $Ca_v1.3$ and processed to assess internalization. Whereas treatment of cells with jasplakinolide alone had no effect on $Ca_v1.3$ distribution, it significantly reduced the promotion of internalization by glutamate, which is apparent from intensity profiles illustrated in insets. The F_c/F_m ratio of 0.75 ± 0.07 ($n = 25$) in the presence of glutamate in jasplakinolide-treated cells, was comparable to the values of 0.67 ± 0.09 ($n = 50$, $P > 0.5$) observed in normal Ringer solution (Fig. 6*B*).

To further establish a link between glutamate-induced suppression of I_{Ca} and internalization of Ca^{2+} channels, we asked whether stabilization of F-actin that prevents channel internalization, is also able to suppress the inhibitory action of glutamate on I_{Ca}. Retinal slices were pre-incubated in Ringer solution containing 10 μM jasplakinolide. A comparison of I_{Ca} traces obtained before and after glutamate application (Fig. 6*C*) shows that stabilization of F-actin resulted in a dramatic

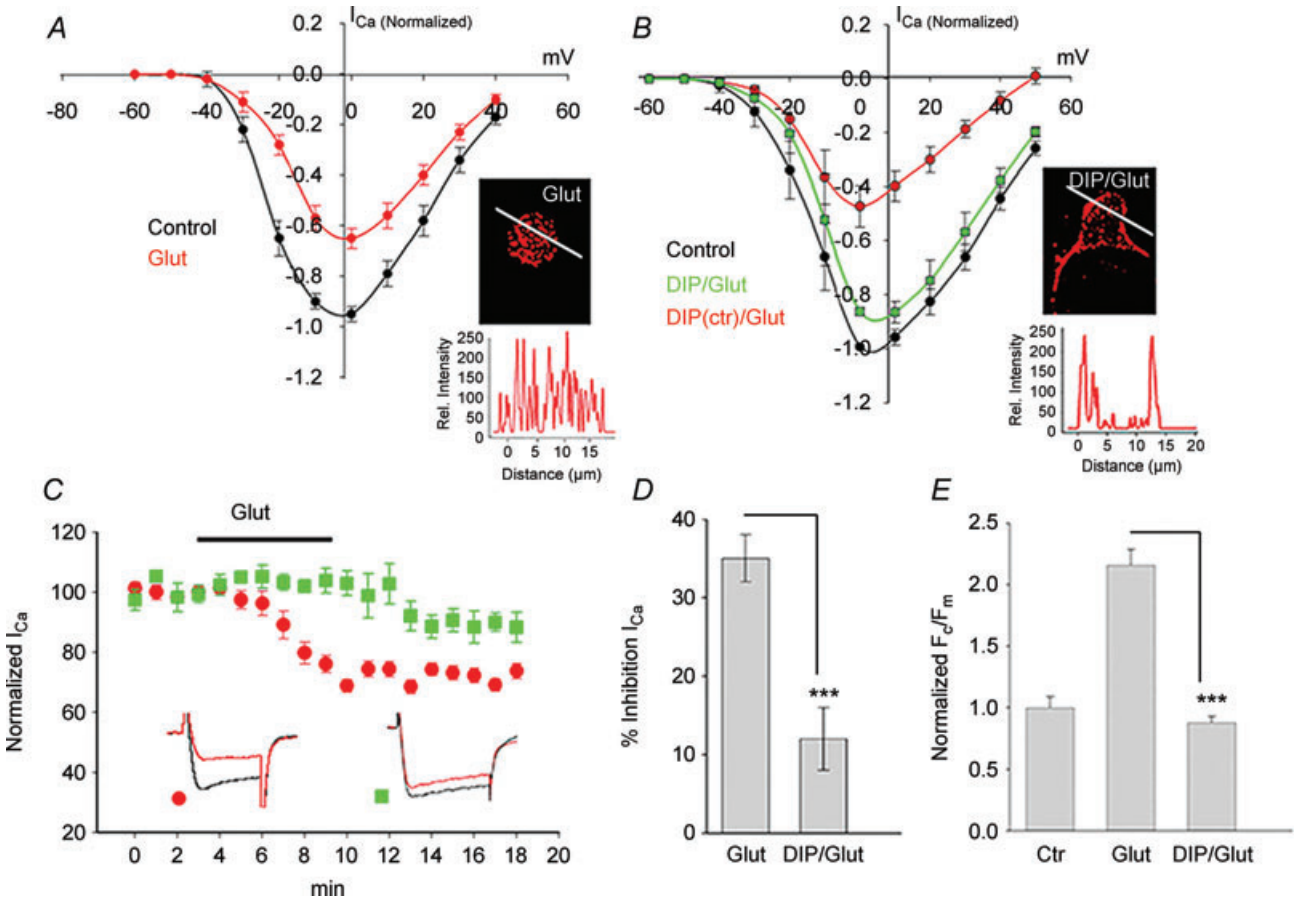

Figure 5. Correlation between channel internalization and inhibition of L-type current by glutamate
A, *I–V* relationships of whole-cell L-type I_{Ca} recorded from ganglion cells in salamander retinal slices from a holding potential of −60 mV to +40 mV in 10 mV increments in control, and in the presence of 100 μM glutamate. *B*, the inhibitory effect of glutamate on I_{Ca} was attenuated in cells pre-treated with DIP, but not with its scrambled analogue (DIP_{ctr}). Immunofluorescence confocal images of cells under indicated conditions are illustrated in insets. *C*, time course of the normalized peak I_{Ca} (mean ± S.E.M.) recorded with the patch pipette containing either DIP or its scrambled inactive form (DIPctr) in the presence of glutamate in the bath solution. The bar graphs summarize the effect of DIP on glutamate-induced inhibition of I_{Ca} (*D*), and internalization of $Ca_v1.3$ (*E*). Values represent mean ± S.E.M. ($n = 7$–16, $P < 0.05$).

decrease in the inhibitory action of glutamate from a mean of $33 \pm 3\%$ to $8 \pm 3\%$ (Fig. 6*C* and *D*, $n = 6$, $P < 0.05$). These findings support the hypothesis that Ca^{2+}-dependent actin reorganization plays a key role in both glutamate-induced internalization and down-regulation of Ca^{2+} channel activity.

Ca^{2+} channel internalization protects RGCs against glutamate excitotoxicity

Ischaemic stress, associated with overactivation of GluRs, excess Ca^{2+} entry into cells and excitotoxic neuronal death have been suggested as the final common pathway in many CNS pathologies including Alzheimer disease, Huntington's disease and ocular disorders such as diabetic retinopathy and glaucoma (Arundine & Tymianski, 2003; Schmidt *et al.* 2008). Although excitotoxicity appears to be primarily triggered by unrestricted Ca^{2+} entry through both voltage-gated LTCCs and iGluR-activated channels, the mechanisms ultimately leading to cell death and those preserving cells from excitotoxic damage are not well understood. We hypothesized that internalization of LTCCs serves as a negative feedback mechanism protecting retinal neurons against glutamate-induced excitotoxicity.

To test this idea, we studied the excitotoxic effect of GluR agonists on RGCs in retinal slices using a live/dead viability assay. Exposure of eyecups to 0.5–1 mM glutamate failed to induce any marked cell death, possibly due to the presence of powerful uptake systems (data not shown). Hence, kainate that is not taken up by glutamate transporters was used to induce cell death in the inner retina. Eyecups were exposed for 30 min to 100 μM kainate, incubated in agonist-free solution for 2–6 h, and examined for cell death by staining with ethidium homodimer. Kainate promoted cell death primarily in the ganglion cell layer, although a few dead cells were also observed in the inner nuclear layer. In salamander retina, the majority of cells in the ganglion cell layer have been characterized as ganglion cells (Lukasiewicz & Werblin, 1988), with only ~4% constituting displaced amacrine cells (Zhang *et al.* 2004). This indicates that kainate targeted predominantly ganglion cells. The number of dead RGCs in control slices and those exposed to kainate (Fig. 7*A* and *B*, arrowheads) were 1.4 ± 0.4 and 5.3 ± 0.9 cells per slice ($n = 30$ slices, $P < 0.005$), respectively. Whereas treatment with DIP alone had no effect on cell death in slices,

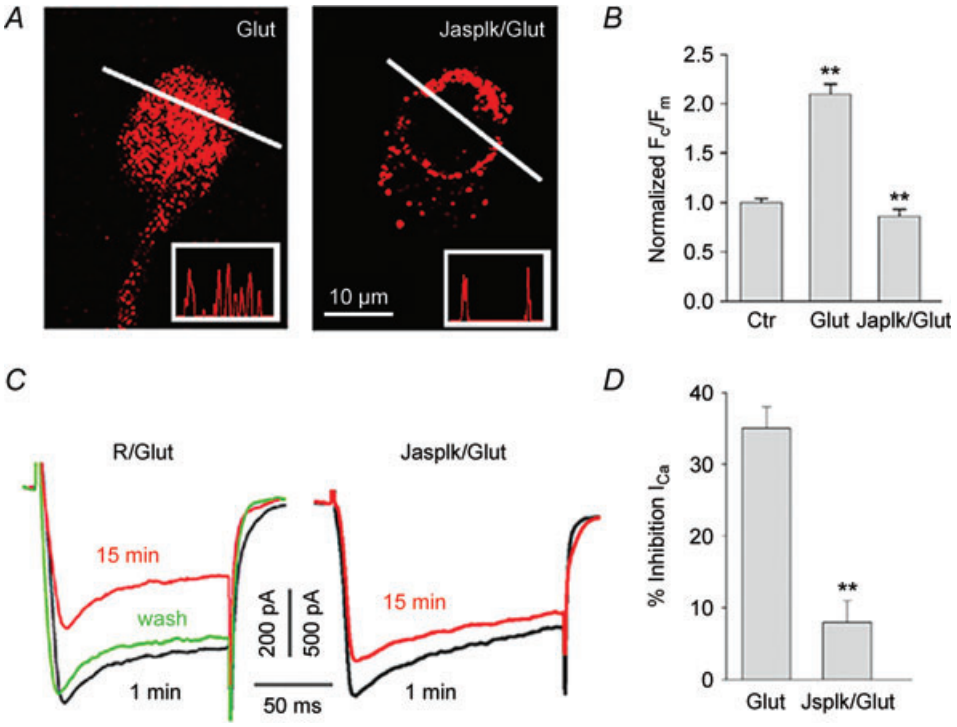

Figure 6. Stabilization of F-actin prevents glutamate-induced $Ca_v1.3$ internalization
A, cells were incubated in either normal Ringer solution (left panel), or in Ringer solution containing 10 μM jasplakinolide (right panel) prior exposing to 100 μM glutamate. *B*, normalized $F_c/F_m \pm$ S.E.M. ($n = 25$–50, $P < 0.005$) measured for jasplakinolide-treated (Jasplk/Glut) and untreated (Glut) cells exposed to glutamate. *C*, traces of L-type I_{Ca} recorded from control (R/Glut) or jasplakinolide-treated (Jasplk/Glut) ganglion cells in salamander retinal slices before (1 min), and after (15 min) application of glutamate. *D*, the bar graph quantifies effect of F-actin stabilization on glutamate-induced inhibition of I_{Ca}. Each bar represents mean $\pm$ S.E.M. ($n = 6$, $P < 0.005$).

it significantly increased the number of kainate-induced dead cells to 13.8 ± 1.2 cells per slice ($n = 16$ slices, $P < 0.005$). Application of the AMPA receptor antagonist CNQX (25 μM) abolished the excitotoxic action of kainate (not shown). Pre-treatment of retinal slices for 30 min with 10 μM jasplakinolide (Fig. 7*E*) modestly increased vulnerability of RGCs ($n = 17$ slices, $P < 0.05$), whereas prior incubation with the F-actin disrupter, cytochalasin D (Fig. 7*D*), markedly reduced kainate-induced cell death ($n = 15$ slices, $P < 0.01$). Quantification of these results is presented as a bar graph in Fig. 7*F*. Collectively, these data support our hypothesis that LTCC internalization acting as negative-feedback protects RGCs against glutamate excitotoxicity.

Discussion

We report here on a novel mechanism whereby internalization of $Ca_v1.3$ LTCC controls glutamate-induced Ca^{2+} overload into retinal neurons. Our data show that activation of iGluRs followed by Ca^{2+} influx and F-actin reorganization are responsible for triggering clathrin-mediated internalization of $Ca_v1.3$ channels. We also provide experimental evidence for the neuroprotective role of $Ca_v1.3$ channel internalization in kainate-induced excitotoxicity, with implications for our understanding of the mechanisms associated with inner retinal dysfunction in several severe blinding diseases.

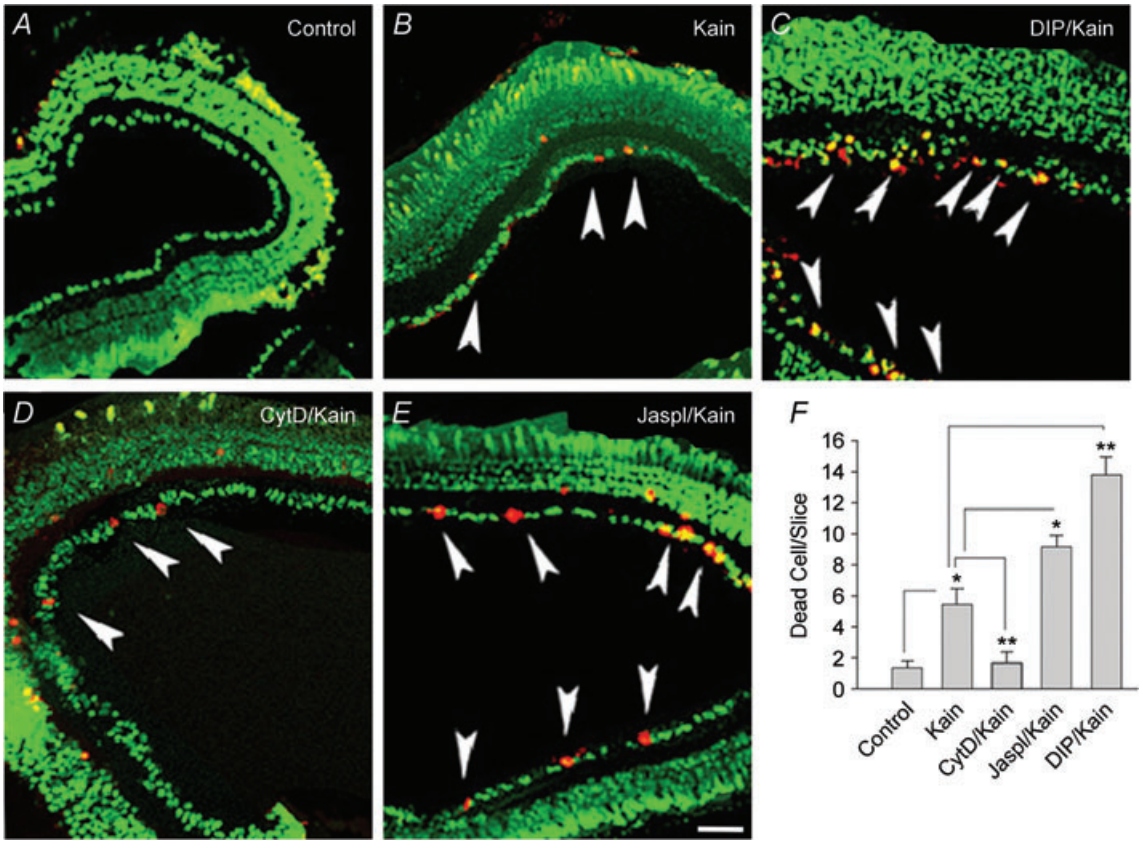

Figure 7. Internalization of $Ca_v1.3$ channels reduced vulnerability of salamander RGCs to kainate-induced excitotoxicity
Live/dead viability assay performed on retinal slices in normal Ringer solution (Control, *A*) exhibited healthy cells (coloured in green) throughout the retina. *B*, exposure of slices for 30 min to 100 μM kainate (Kain) promoted cell death in the ganglion cell layer (GCL) (arrowheads) and also few cells in the inner nuclear layer. *C*, prior incubation of slices for 30–40 min with 50 μM DIP (DIP/Kain) significantly enhanced kainate-induced cell death in the GCL. *D*, pre-incubation of slices with 10 μM cytochalasin D (CytD/Kain) markedly reduced kainate-induced RGC death. *E*, in contrast, stabilization of F-actin by 10 μM jasplakinolide (Jaspl/Kain) increased the number of kainate-induced dead cells (*E*). *F*, quantification summarizes these data indicating the role of endocytosis and cytoskeletal dynamics in excitotoxic RGC death. Each bar represents the number of dead cells per slice ± S.E.M. ($n = 16$–20 slices, $^*P < 0.05$; $^{**}P < 0.01$; 3 independent experiments). Statistical analysis was performed using ANOVA, followed by Tukey's *post hoc* test. Only cells in the GCL were considered for statistical analysis. Calibration bar, 50 μm.

Internalization of $Ca_v1.3$ is mediated by Ca^{2+} entry and F-actin reorganization

In vertebrate retinal amacrine and ganglion cells, activation of iGluRs induces Ca^{2+} influx through Ca^{2+}-permeable AMPA/KA and NMDA-gated channels as well as voltage-operated Ca^{2+} channels activated by incipient depolarization (Lu *et al.* 1996; Akopian *et al.* 2006; Hartwick *et al.* 2008). In addition, Ca^{2+}-permeable store-operated channels (SOC) might be transiently activated following kainate-induced depletion of ER stores. Activation of G protein-coupled group III mGluRs, on the other hand, elevates $[Ca^{2+}]_i$ by triggering Ca^{2+} release from IP_3-sensitive and/or ryanodine-sensitive internal stores. Three lines of evidence argue that Ca^{2+} entry through Ca^{2+}-permeable iGluRs and voltage-gated LTCCs, rather than its release from internal stores, is responsible for glutamate-induced internalization of $Ca_v1.3$: (i) the effect of glutamate was prevented by removal of Ca^{2+} from external solution, (ii) activation of group III mGluRs by L-AP4, which stimulates Ca^{2+} release from IP_3-sensitive internal stores in retinal neurons (Shen & Slaughter, 1998), failed to induce $Ca_v1.3$ internalization, (iii) depletion of ryanodine and IP_3-sensitive internal stores by thapsigargin, or block of Ca^{2+} entry via SOC and/or TRP channels by 2-APB (Maruyama *et al.* 1997; Szikra *et al.* 2008), had no effect on glutamate-induced internalization. We therefore propose that the effect of Ca^{2+} is mediated by F-actin reorganization, as stabilization of F-actin by jasplakinolide prevented glutamate-mediated $Ca_v1.3$ internalization in presumed RGCs. This idea is supported by our previous findings indicating that Ca^{2+} influx causes actin depolymerization, which in turn reduces voltage-operated Ca^{2+} entry in salamander RGCs (Schubert & Akopian, 2004; Cristofanilli & Akopian, 2006). Similar dependence of $Ca_v1.3$ internalization on Ca^{2+} influx and baseline $[Ca^{2+}]_i$ has been shown recently to mediate glucose-evoked insulin release in pancreatic β-cells (Huang *et al.* 2004). Taken together, these observations suggest that regulated endocytosis of LTCCs serves as a powerful negative feedback mechanism to limit Ca^{2+} loads imposed upon cells during sustained depolarization.

Although previous studies reported downregulation of L-type I_{Ca} in RGCs by iGluR activation (Taschenberger & Grantyn, 1998; Shen & Slaughter, 1998), it is not known whether such modulation is specific for channel subtype, or if the reduction in channel activity is accompanied by alterations in the number of channels in the plasma membrane. We show that iGluR agonists selectively target $Ca_v1.3$ channels without affecting the subcellular distribution of $Ca_v1.2$, suggesting that LTCCs in the retina can undergo subtype-selective modulation. A potential mechanism for this process might involve the ProSAP/Shank family of scaffolding proteins which link GluRs and the C-terminal of the $Ca_v1.3$ channels to the PSD-95/SAP90 complex, which act as a scaffold for various neurotransmitter receptors, ion channels, or other signaling molecules, and is coupled both to regulators of F-actin and the endocytic machinery via dynamin (Okamoto *et al.* 2001; Olson *et al.* 2005). The stability of plasma membrane $Ca_v1.2$ clusters during glutamatergic stimulation was displayed in central neurons, in which both targeting and expression of $Ca_v1.2$ channels failed to change following activation of NMDARs (Di Biase *et al.* 2009; but see Green *et al.* 2007). We therefore propose that glutamate-induced Ca^{2+} entry disrupts F-actin, which in turn triggers removal of $Ca_v1.3$ channels from plasma membrane by endocytosis.

Internalization underlies an inhibition of L-type Ca^{2+} channel activity by glutamate

Our electrophysiological data strongly indicate that dynamin-dependent internalization of $Ca_v1.3$ channels is the major underlying mechanism for glutamate-induced inhibition of L-type currents in salamander RGCs. This conclusion is supported by the following lines of evidence: (i) both glutamate-induced internalization of $Ca_v1.3$ channels and inhibition of L-type currents in RGCs were attenuated by dynamin inhibition; (ii) removal of extracellular Ca^{2+}, or strong buffering of internal Ca^{2+} by BAPTA, abolished the $Ca_v1.3$ channel internalization and suppressed the inhibitory action of glutamate on I_{Ca}; (iii) stabilization of F-actin by jasplakinolide significantly reduced the effect of glutamate on both I_{Ca} inhibition and channel internalization. Given that AMPARs do not cycle in intact light-adapted retinas (Xia *et al.* 2006), it is unlikely that DIP interfered with internalization of AMPARs (Luscher *et al.* 1999). Our results are in agreement with the generally recognized role of F-actin in controlling endocytosis and the delivery of ion channel proteins into and out of the plasma membrane (Tombler *et al.* 2006; Lanzetti, 2007).

Implications for glutamate-induced excitotoxicity

Overstimulation of GluRs followed by excess Ca^{2+} entry is thought to be associated with cellular degeneration, remodelling and cell death in many ocular pathologies such as diabetic retinopathy and glaucoma (Tezel & Wax, 2004; Osborne *et al.* 2008), whereas antagonism of L-type channels was shown to exert protective effects (Koseki *et al.* 2008; Sakamoto *et al.* 2009). Results presented in this study are consistent with earlier reports in central neurons demonstrating a link between endocytosis or F-actin dynamics and excitotoxic cell death (Furukawa *et al.* 1997). The proposed mechanism may also be helpful for understanding the controversy regarding involvement of glutamate excitotoxicity in RGC

death in glaucoma, as several studies failed to detect substantial elevations in glutamate levels in the glaucomatous eye (Salt & Cordeiro, 2006). Our results suggest that the excitotoxic damage caused by initial ischaemia is not determined exclusively by elevated levels of intraretinal glutamate, but also depends upon: (i) the relative proportion of $Ca_v1.3$ (over $Ca_v1.2$) channels within a given cell, (ii) the functional state of the endocytic machinery, and (iii) the actin cytoskeleton dynamics. Recent studies demonstrated that LTCC blockers reduce intraocular pressure in the primate and human eye (Tian *et al.* 2000; Wang *et al.* 2008), stabilize the progression of glaucoma (Mikheytseva *et al.* 2004), induce an improvement in visual field parameters in glaucoma patients (Luksch *et al.* 2005; Koseki *et al.* 2008), and protect RGCs against hypoxia/ischaemia (Uemura & Mizota, 2008; Sakamoto *et al.* 2009). Conversely, facilitation of Ca^{2+} influx through LTCCs is likely to worsen the clinical picture via Ca^{2+} overloads in RGCs. It is therefore plausible that LTCC internalization plays a protective role by reducing excessive excitation and by preserving the metabolic capital of the cell that would have been expended combating Ca^{2+} overloads. Our findings, therefore, are likely to point at a universal mechanism that underlies neuroprotection in degenerative diseases in the retina and across the CNS.

In summary, we show that activation of iGluRs triggers clathrin-mediated selective internalization of $Ca_v1.3$ LTCC in a subset of retinal amacrine and ganglion neurons. This process is mediated by Ca^{2+}-dependent F-actin reorganization. This internalization mechanism may serve as a negative feedback during light–dark adaptation to modulate the excitability of inner retinal circuits and to ensure constant output under different illumination conditions. Our data also suggest that internalization of LTTCs could control glutamate-induced deregulation of Ca^{2+} homeostasis.

References

Akopian A, Szikra T, Cristofanilli M & Krizaj D (2006). Glutamate-induced Ca^{2+} influx in third-order neurons of salamander retina is regulated by the actin cytoskeleton. *Neuroscience* **138**, 17–24.

Akopian A & Witkovsky P (2002). Calcium and retinal function. *Mol Neurobiol* **25**, 95–114.

Arundine M & Tymianski M (2003). Molecular mechanisms of calcium-dependent neurodegeneration in excitotoxicity. *Cell Calcium* **34**, 325–337.

Bech-Hansen NT, Naylor MJ, Maybaum TA, Sparkes RL, Koop B, Birch DG Bergen AA, Prinsen CF, Polomeno RC, Gal A, Drack AV, Musarella MA, Jacobson SG, Young RS & Weleber RG (2000). Mutations in NYX, encoding the leucine-rich proteoglycan nyctalopin, cause X-linked complete congenital stationary night blindness. *Nat Genet* **26**, 319–323.

Busquet P, Khoi Nguyen N, Schmid E, Tanimoto N, Seeliger MW, Ben-Yosef T, Mizuno F, Akopian A, Striessnig J & Singewald N (2009). $Ca_V1.3$ L-type Ca^{2+} channels modulate depression-like behaviour in mice independent of deaf phenotype. *Int J Neuropsychopharmacol* **11**, 1–15.

Choi DW (1988). Glutamate neurotoxicity and diseases of the nervous system. *Neuron* **1**, 623–634.

Cristofanilli M & Akopian A (2006). Calcium channel and glutamate receptor activities regulate actin organization in salamander retinal neurons. *J Physiol* **575**, 543–554.

Cristofanilli M, Mizuno F & Akopian A (2007). Disruption of actin cytoskeleton causes internalization of $Ca_v1.3$ (alpha 1D) L-type calcium channels in salamander retinal neurons. *Mol Vis* **13**, 1496–1507.

Di Biase V, Obermair GJ, Szabo Z, Altier C, Sanguesa J, Bourinet E & Flucher BE (2009). Stable membrane expression of postsynaptic $Ca_V1.2$ calcium channel clusters is independent of interactions with AKAP79/150 and PDZ proteins. *J Neurosci* **28**, 13845–13855.

Firth SI, Morgan IG, Boelen MK & Morgans CW (2001). Localization of voltage-sensitive L-type calcium channels in the chicken retina. *Clin Exp Ophthalmol* **29**, 183–187.

Furukawa K, Fu W, Li Y, Witke W, Kwiatkowski DJ & Mattson MP (1997). The actin-severing protein gelsolin modulates calcium channel and NMDA receptor activities and vulnerability to excitotoxicity in hippocampal neurons. *J Neurosci* **17**, 8178–8186.

Green EM, Barrett CF, Bultynck G, Shamah SM & Dolmetsch RE (2007). The tumor suppressor eIF3e mediates calcium-dependent internalization of the L-type calcium channel $Ca_V1.2$. *Neuron* **55**, 615–632.

Hartwick AT, Hamilton CM & Baldridge WH (2008). Glutamatergic calcium dynamics and deregulation of rat retinal ganglion cells. *J Physiol* **586**, 3425–3446.

Henderson D, Doerr TA, Gottesman J & Miller RF (2001). Calcium channel immunoreactivity in the salamander retina. *Neuroreport* **12**, 1493–1499.

Huang L, Bhattacharjee A, Taylor JT, Zhang M, Keyser BM, Marrero L & Li M (2004). $[Ca^{2+}]_i$ regulates trafficking of $Ca_v1.3$ (α_{1D} Ca^{2+} channel) in insulin-secreting cells. *Am J Physiol Cell Physiol* **286**, C213–C221.

Jarvis SE & Zamponi GW (2007). Trafficking and regulation of neuronal voltage-gated calcium channels. *Curr Opin Cell Biol* **19**, 474–482.

Kamphuis W & Hendriksen H (1998). Expression patterns of voltage-dependent calcium channel alpha 1 subunits (α_{1A}–α_{1E}) mRNA in rat retina. *Brain Res Mol Brain Res* **55**, 209–220.

Koseki N, Araie M, Tomidokoro A, Nagahara M, Hasegawa T, Tamaki Y & Yamamoto S (2008). A placebo-controlled 3-year study of a calcium blocker on visual field and ocular circulation in glaucoma with low–normal pressure. *Ophthalmology* **115**, 2049–2057.

Lanzetti L (2007). Actin in membrane trafficking. *Curr Opin Cell Biol* **19**, 453–458.

Le Roy C & Wrana JL (2005). Clathrin- and non-clathrin-mediated endocytic regulation of cell signalling. *Nat Rev Mol Cell Biol* **6**, 112–126.

Lu YM, Yin HZ, Chiang J & Weiss JH (1996). Ca permeable AMPA/kainite and NMDA channels: high rate of Ca influx underlies potent induction of injury. *J Neurosci* **16**, 5457–5465.

Lukasiewicz P & Werblin F (1988). A slowly inactivating potassium current truncates spike activity in ganglion cells of the tiger salamander retina. *J Neurosci* **12**, 4470–4481.

Luksch A, Rainer G, Koyuncu D, Ehrlich P, Maca T, Gschwandtner ME, Vass C & Schmetterer L (2005). Effect of nimodipine on ocular blood flow and colour contrast sensitivity in patients with normal tension glaucoma. *Br J Ophthalmol* **89**, 21–25.

Lüscher C, Xia H, Beattie EC, Carroll RC, von Zastrow M, Malenka RC & Nicoll RA (1999). Role of AMPA receptor cycling in synaptic transmission and plasticity. *Neuron* **24**, 649–658.

Maruyama T, Kanaji T, Nakade S, Kanno T & Mikoshiba K (1997). 2APB, 2-aminoethoxydiphenyl borate, a membrane-penetrable modulator of Ins(1,4,5)P_3-induced Ca^{2+} release. *J Biochem* **122**, 498–505.

Mikheytseva IN, Kashintseva LT, Krizhanovsky GN, Kopp OP & Lipovetskaya EM (2004). The influence of the calcium channel blocker verapamil on experimental glaucoma. *Int Ophthalmol* **25**, 75–79.

Morgans CW (1999). Localization of the 1F calcium channel subunit in the rat retina. *Invest Ophthalmol Vis Sci* **42**, 2414–2418.

Okamoto PM, Gamby C, Wells D, Fallon J & Vallee RB (2001). Dynamin isoform-specific interaction with the shank/ProSAP scaffolding proteins of the postsynaptic density and actin cytoskeleton. *J Biol Chem* **276**, 48458–48465.

Olson PA, Tkatch T, Hernandez-Lopez S, Ulrich S, Ilijic E, Mugnaini E, Zhang H, Bezprozvanny I & Surmeier DJ (2005). G-protein-coupled receptor modulation of striatal $Ca_V1.3$ L-type Ca^{2+} channels is dependent on a Shank-binding domain. *J Neurosci* **25**, 1050–1062.

Osborne NN, Wood JP, Chidlow G, Bae JH, Melena J & Nash MS (2008). Ganglion cell death in glaucoma: what do we really know? *Brit J Ophthalmol* **83**, 980–986.

Sakamoto K, Kawakami T, Shimada M, Yamaguchi A, Kuwagata M, Saito M, Nakahara T & Ishii K (2009). Histological protection by cilnidipine, a dual L/N-type Ca^{2+} channel blocker, against neurotoxicity induced by ischemia-reperfusion in rat retina. *Exp Eye Res* **88**, 974–982.

Salt TE & Cordeiro MF (2006). Glutamate excitotoxicity in glaucoma: throwing the baby out with the bathwater? *Eye* **20**, 730–731.

Sattler R & Tymianski M (2001). Molecular mechanisms of glutamate receptor-mediated excitotoxic neuronal cell death. *Mol Neurobiol* **24**, 107–129.

Schmidt KG, Bergert H & Funk RH (2008). Neurodegenerative diseases of the retina and potential for protection and recovery. *Curr Neuropharmacol* **6**, 164–178.

Schubert T & Akopian A (2004). Actin filaments regulate voltage-gated ion channels in salamander retinal ganglion cells. *Neuroscience* **125**, 583–590.

Shen W & Slaughter MM (1998). Metabotropic and ionotropic glutamate receptors regulate calcium channel currents in salamander retinal ganglion cells. *J Physiol* **510**, 815–828.

Strom TM, Nyakatura G, Apfelstedt-Sylla E, *et al.* (1998). An L-type calcium-channel gene mutated in incomplete X-linked congenital stationary night blindness. *Nat Genet* **19**, 260–263.

Sucher NJ, Lipton SA & Dreyer EB (1997). Molecular basis of glutamate toxicity in retinal ganglion cells. *Vision Res* **37**, 3483–3493.

Szikra T, Cusato K, Thoreson WB, Barabas P, Bartoletti TM & Krizaj D (2008). Depletion of calcium stores regulates calcium influx and signal transmission in rod photoreceptors. *J Physiol* **586**, 4859–4875.

Szikra T & Krizaj D (2006). The dynamic range and domain-specific signals of intracellular calcium in photoreceptors. *Neuroscience* **141**, 143–155.

Taschenberger H & Grantyn R (1998). Interaction of calcium-permeable non-*N*-methyl-D-aspartate receptor channels with voltage-activated potassium and calcium currents in rat retinal ganglion cells *in vitro*. *Neuroscience* **84**, 877–896.

Taylor WR & Morgans C (1998). Localization and properties of voltage-gated calcium channels in cone photoreceptors of *Tupaia belangeri*. *Vis Neurosci* **15**, 541–552.

Tezel G & Wax MB (2004). Hypoxia-inducible factor 1α in the glaucomatous retina and optic nerve head. *Arch Ophthalmol* **122**, 1348–1356.

Thoreson WB & Witkovsky P (1999). Glutamate receptors and circuits in the vertebrate retina. *Prog Retin Eye Res* **18**, 765–810.

Tian B, Geiger B, Epstein DL & Kaufman PL (2000). Cytoskeletal involvement in the regulation of aqueous humor outflow. *Invest Ophthalmol Vis Sci* **41**, 619–623.

Tombler E, Cabanilla NJ, Carman P, Permaul N, Hall JJ, Richman RW, Lee J, Rodriguez J, Felsenfeld DP, Hennigan RF & Diversé-Pierluissi MA (2006). G protein-induced trafficking of voltage-dependent calcium channels. *J Biol Chem* **281**, 1827–1839.

Uemura A & Mizota A (2008). Retinal concentration and protective effect against retinal ischemia of nilvadipine in rats. *Eur J Ophthalmol* **18**, 87–93.

Wang RF, Gagliuso DJ & Podos SM (2008). Effect of flunarizine, a calcium channel blocker, on intraocular pressure and aqueous humor dynamics in monkeys. *J Glaucoma* **17**, 73–78.

Wigge P, Kohler K, Vallis Y, Doyle CA, Owen D, Hunt SP & McMahon HT (1997). Amphiphysin heterodimers: potential role in clathrin-mediated endocytosis. *Mol Biol Cell* **8**, 2003–2015.

Xia Y, Carroll RC & Nawy S (2006). State-dependent AMPA receptor trafficking in the mammalian retina. *J Neurosci* **26**, 5028–5036.

Zhang J, Yang Z & Wu SM (2004). Immuocytochemical analysis of spatial organization of photoreceptors and amacrine and ganglion cells in the tiger salamander retina. *Vis Neurosci* **21**, 157–166.

Zhou ZJ & Fain GL (1995). Neurotransmitter receptors of starburst amacrine cells in rabbit retinal slices. *J Neurosci* **15**, 5334–5345.

Author contributions

F.M.: collection, analysis and interpretation of data; final approval of the manuscript. P.B. and D.K.: drafting and revising the manuscript, final approval of the manuscript; A.A.: conception and design of the experimental protocol; collection, analysis and interpretation of data; drafting and revising the manuscript; final approval of the manuscript.

Acknowledgement

We thank Dr J. Striessnig and A. M. Rajadhyaksha for critically reading the manuscript. This research was supported by NIH grants EY13870 to D.K. and EY12497 to A.A. P.B. wishes to acknowledge support from the Institute of Biomolecular Chemistry, Hungarian Academy of Sciences, Budapest, Hungary.

Author's present address

F. Mizuno: Department of Neurobiology, Duke University Medical Center. Durham, NC 27710, USA.